

Epitaxial Growth of Sputtered Ultra-thin NbN Layers and Junctions on Sapphire

J-C. Villegier, S. Bouat, P. Cavalier, R. Setzu, R. Espiau de Lamaëstre, C. Jorel, Ph. Odier, B. Guillet, L. Mechin, M. P. Chauvat, P. Ruterana

Abstract—High crystalline quality of ultra-thin NbN layers and of NbN-MgO-NbN tri-layers, epitaxially grown by DC-magnetron sputtering in the superconducting B1-cubic phase has been achieved in a reproducible way on three different orientations of sapphire substrates i.e. R-, A- and M-planes. Significant improvements such as higher T_c , higher J_c and lower resistivity have been obtained by growing untwined (110) oriented NbN layers on M-plane orientation of sapphire. Uniform, low roughness, 3-5 nm thick films with T_c above 12 K and J_c above 5 MA/cm² at 4.2K were obtained. Characterizations by TEM, AFM and X-Ray diffraction evidence that growth of untwined NbN on M-plane lead to a better epitaxy in comparison with twinned films observed on other sapphire orientations. We observe that the reduction of the substrate temperature from 600°C to 300°C during the deposition of NbN or NbN-MgO-NbN layers thicker than 20 nm prevents the nucleation of the competing HCP NbN phase. Moreover, 1.5 nm thick AlN or MgO over-layers sputtered in-situ prevent ultra-thin NbN films degradation through aging. The formation of Nb₂N_yO_{5-x} (~2.2 nm) at the unprotected NbN surface and of interfacial NbO (~0.7 nm) native oxides has been observed by XPS. It is forecasted that such improvements in ultra-thin NbN films deposited uniformly on 3 and 4 inch sapphire wafers is a key in the future development of superconducting single photon detectors, THz HEB mixers and also in low noise quantum analogical and digital Josephson devices.

Index Terms— Josephson epitaxial junctions, Niobium nitride compounds, Superconducting filaments and wires, Superconducting epitaxial layers, Thin films.

I. INTRODUCTION

HIGH structural quality and high reliability in the single crystal deposition of ultra-thin films (3 to 20 nm thick) of the superconducting B1-cubic phase of niobium nitride (NbN) [1-2] have been shown to be mandatory for the development of efficient infrared superconducting nanowire single photon detectors (SNSPD), counters, spectrometers [3-5] and of large IF-bandwidth THz hot electron mixers [6].

Manuscript received 26 August 2008.

This work was supported in part by the Grant *EC Sinfonia NMP4-CT-2005-16433* and by the Grant *'HyperSCAN' ANR T-COM-06-023*.

S. Bouat, P. Cavalier, R. Setzu and J-C. Villegier are with the CEA, Institute of Nanosciences and Cryogenics, SPSMS, CEA-Grenoble, 38054 Grenoble-Cedex-9, France (corresponding author J-C Villegier, phone: 33+438783587; fax: 33+438785096; e-mail: jean-claude.villegier@cea.fr).

R. Espiau de Lamaëstre is with CEA-Leti-MINATEC, 38054 Grenoble, Fr.

C. Jorel is with Leti-MINATEC/CNRS-LTM, 38054 Grenoble-Cdx-9, Fr.

Ph. Odier is with the CNRS, Institut Néel, 38042 Grenoble-Cedex, Fr.

B. Guillet, L. Mechin are with GREYC(UMR 6072) – CNRS – ENSICAEN – Univ. Caen Basse-Normandie; M.P. Chauvat and P. Ruterana with CIMAP(UMR 6252) – CNRS – CEA - ENSICAEN, 6 bd Marechal Juin, 14050 Caen-Cedex, Fr.

Quantum analog and digital integrated circuits performances should also be increased by using better quality NbN junction tri-layers, with large characteristic voltage ($I_c R_N$) and large operating temperatures. This should be achieved through the improvement of NbN crystalline quality of junction electrodes and barrier, which is linked to a reduction in London penetration depth value and to an increase in energy gap [7-9].

Efforts devoted to the NbN layer growth aim at improving the critical temperature T_c and the critical current density J_c , but also the long term reliability and the reproducibility of few nanometer thick layers covering uniformly a large area wafer. Long term reliability of very thin layers is an issue, which would make NbN films attractive among other superconducting metals and compound materials such as Nb or YBCO, which are more sensitive to oxygen in- and out-diffusion and sensitive to chemical degradations.

The choice of substrate is critical in regards to its crystalline, electronic and physicochemical properties to be matched with the NbN ones [2]. Among single crystal wafers, Silicon, Sapphire and MgO substrates are generally considered first. Cubic MgO substrates give the best match with the B1 nitride structure leading to an epitaxial relationship that we observed even when the substrate is maintained at room temperature during the NbN sputter deposition [10]. By characterizing the epitaxial growth and the superconducting transport properties of NbN nanowires on three different orientations of sapphire we intend to bring new arguments for considering M-plane sapphire as the best compromise for achieving uniform superconducting performances in long nanowires, which is a critical issue in SSPDs [11]. We also take into account that MgO substrates are expensive and hydrophilic, while it would be difficult in most of the sputtering systems to deposit uniformly a suitable crystalline template on silicon wafers after in-situ removing of the SiO₂ surface oxide without damage.

II. NBN FILM DEPOSITION CONDITIONS

NbN films were deposited on the R-, A- and M- plane orientations of epitaxially polished (3 or 4 inches in diameter) sapphire substrates, from Kyocera. MgO (100) oriented substrates were also used for some of the comparisons. The NbN films were grown by reactive DC-magnetron sputtering (Alcatel-650 equipment) done at about 600°C substrate temperature, as we described previously [10]. Very thin NbN layers were obtained in a reproducible way by controlling both the nitrogen-argon reactive plasma sputtering conditions (total pressure $P_{tot}=1.88 \cdot 10^{-2}$ mbar; ~10% N₂ partial pressure; 4A as cathode dc current) and the number of turns in the rotation of the substrate holder above the 6 inch diameter Nb target. In order to prevent their subsequent degradation by oxidation in

atmosphere, the NbN films are generally covered by an in-situ AlN layer (~1.5nm thick) that are RF-sputtered after cooling the wafer to room temperature. Alternative MgO, TaN or bi-layers were also sputtered, for comparison some of the characterized over-layers are presented in Table 1.

A significant improvement in the NbN film quality on M-plane orientation of sapphire versus R-plane or A-plane (i.e. higher critical temperature (Tc), higher current density at 4.2K (Jc) and lower resistivity at 300K and 20K) has been observed in a first attempt by growing simultaneously NbN on the three different wafer cuts [12-13].

New layers including thinner films, over-layers and multi-layers have been grown for this study (on separate runs) on the three sapphire cuts, 3 or 4 inch in diameter for characterizing and comparing their typical structural features. Films have been patterned to study their superconducting properties.

III. STRUCTURAL CHARACTERIZATION

A. X-Ray Diffraction and Reflectivity Characterizations

The microstructure of NbN films grown on the three sapphire cut substrates has been examined by both symmetric and asymmetric X-ray diffraction using a Cu K α source, [Siefert texture apparatus] in the Schulz configuration, indicating pike poles as shown in figure 1. The observation of diffraction peaks gives insight on the in-plane and perpendicular orientation of the NbN film. This confirms that NbN are both (110) oriented and un-twinned on M-plane, while films are twinned around the (135) orientation on top of R-plane sapphire. Moreover NbN films are also found to be twinned and (111) oriented on the A-plane sapphire substrates.

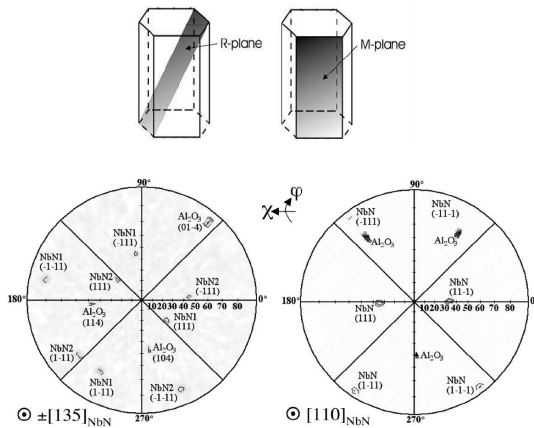


Fig. 1. X-ray pole figures of cubic NbN Bragg reflections on sapphire R-plane and M-plane cuts. Left: on R-plane sapphire ($2q=35.03^\circ$), the two twinning variants are noted NbN1 and NbN2. Right: on M-plane sapphire. The contour lines underline the weak NbN diffraction signal. Diffraction indicates the improved NbN (110) oriented un-twinned on M-plane.

The NbN layer thickness and mean roughness were measured by X-ray reflectivity at low angle, using a Philips X'Pert for the data acquisition and the Paratt fit [16] applied to the experimental data.

TABLE 1 NbN LAYERS AND OVER-LAYERS STUDIED

	Sapphire plane cut	Overlayer	NbN thicknesses	Resistivity (300K)	Tc (K)
A	R- plane	AlN (1.5 nm)	5.2 nm	138 $\mu\Omega$.cm	12.4
B	A-plane	MgO (2.2 nm)	6.8 nm	124 $\mu\Omega$.cm	13.4
C	M-plane	AlN (1.5 nm)	4.35 nm	102 $\mu\Omega$.cm	13.3
D	M-plane	Nb ₂ O _{5-x} (2.2 nm) native oxide	2.86 nm	142 $\mu\Omega$.cm	11.7

Figure 2 presents good fits obtained for determining the thickness of ultra-thin films of 4.35 nm (Tc=13.3K) and 2.86 nm (Tc=11.7K) using the Paratt fit applied to NbN reflectivity versus tilt angle (~ Q vector) at low angles (few degrees).

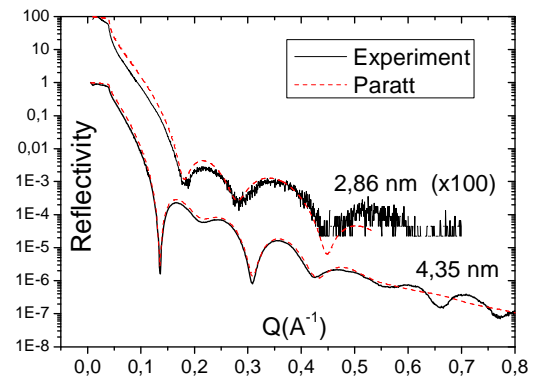


Fig. 2. X-ray reflectivity determination of the thicknesses of two ultra-thin NbN films as a function of the sample tilt at grazing angles (diffusion vector Q) and fit with the Paratt extraction model [16].

Thicknesses can be determined with an accuracy of about +/- 5% even when applied to ultra-thin NbN layers of Figure 2 covered by either an in-situ deposited over-layer or by the native surface oxide of NbN as described in Table 1.

B. HR-TEM Characterization

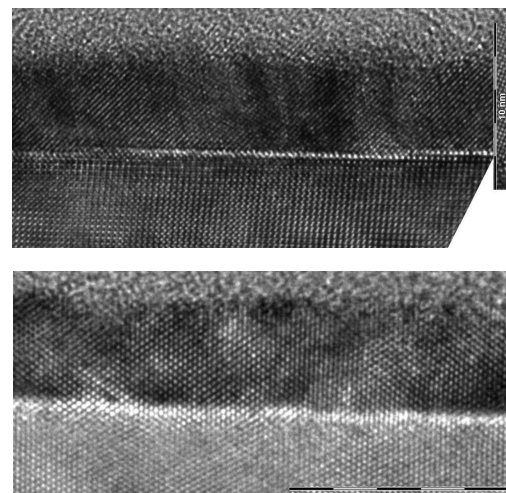


Fig. 3. TEM cross-section observation (rule is 10nm) of (top) sample A in Table.1, showing twinned (135) oriented NbN on R-plane sapphire and (bottom) sample C showing NbN (110) untwinned on M-plane.

High Resolution Transmission Electron Microscopy (HR-TEM) cross-section images of NbN samples A,B,C in Table.1, grown on R-, A- and M-plane sapphire cut substrates fully

confirmed the interpretation of the XRD measurements on the NbN crystalline orientations [12-13] and on the twinning domains observed, except for growth on M-plane. High resolution microscopy presented in Figure 3 evidences the good crystalline quality but the different orientations of NbN observed on M-plane versus R-plane sapphire cuts. There is more insight obtained from TEM and AFM. There are regular surface steps and terraces on R-plane (step distance $d_{\text{ter}} \sim 1$ nm) and on A-plane ($d_{\text{ter}} \sim 7$ nm) but M-plane looks flat without any step on it. NbN strain relaxed grains are found well aligned in-plane on top of the M-plane sapphire, while twinned domains with random sizes on R- and A-plane sapphire are found with some misoriented grains [18].

C. X-Photoelectron Spectroscopy Characterization

An ultra-thin NbN (2.86 nm thick) film grown on M-plane sapphire substrate labelled *sample D* in Table 1, intentionally not covered by any over-layer but by its native oxide grown at room temperature in air, has been analysed by X-ray Photoelectron Spectroscopy (XPS) and surface scanning at CEA-Minatec. The thickness-dependent chemical properties of surface oxy-nitrides are studied for determining the local origin of detrimental NbN defects acting on the ultra-thin films long term degradation *i.e.* square resistance increase and T_c decrease. Nb^{3d3} , Nb^{3d5} , N^{1s} , C^{1s} , atom orbit signatures and their energy shift have been studied as described elsewhere [19]. NbN samples A, B, C in table 1, covered by AlN, MgO over-layers have also been studied by XPS in order to understand their better stability under aging.

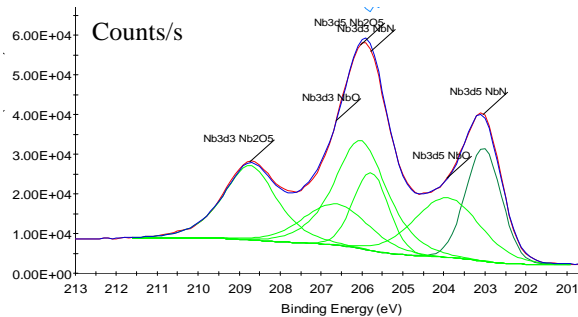


Fig. 4. XPS spectrum of the Nb^{3d3} and Nb^{3d5} pikes intensity versus binding energy for a 2.9 nm NbN covered by its native oxy-nitride (*sample D*), after de-convolving the presence of a Nb_2O_5 (1.8 nm thick) surface compound dominant and of a ~ 0.7 nm NbO compound at the NbN interface.

XPS energy spectrum of the Nb^{3d3} and Nb^{3d5} from NbN *sample D* (2.86 nm thick) covered by its native oxy-nitride after one month storage in air, looks very uniform at a sub-micrometer to cm scales and is presented in Figure 4. After pike de-convolving we observed the presence of a dominant Nb_2O_5 (1.8 nm thick) surface compound and of a ~ 0.7 nm thick NbO compound at the NbN interface. The total surface oxy-nitride thickness (~ 2.5 nm) observed by XPS is found a bit thicker than that taken from the measurement of X-ray reflectivity (1.8 nm), made only one day after sample deposition. However in the X-ray Paratt fit, interface layer has not been ascribed to a defined compound. We also observed a 10% increase in NbN square resistance value between the two measurements. In opposite, we observed that in-situ sputtered

1.5 nm thick, AlN or MgO over-layers efficiently prevent from aging effects and formation of $\text{Nb}_2\text{N}_y\text{O}_{5-x}$ and NbO native oxy-nitrides [19].

IV. NBN FILMS AND FILAMENTS TRANSPORT PROPERTIES

The superior transport performances of NbN layers grown on M-plane sapphire in comparison with the ones grown on R-plane (or on A-plane) measured by the four-point method on un-patterned films are presented in Figure 5: the critical temperature T_c is increased and the resistivity is decreased when using M-plane versus R-plane sapphire for NbN thickness in the range of 2.5 nm to 10 nm.

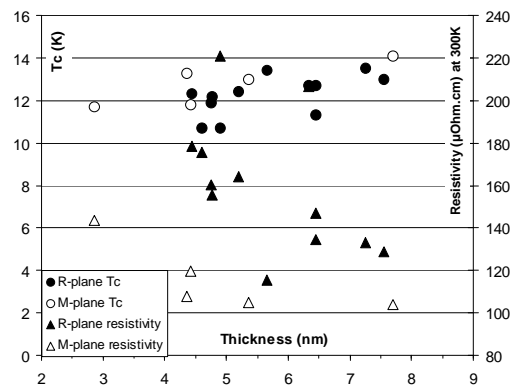


Fig. 5. Measurement of the critical temperature T_c and room temperature resistivity versus NbN film thickness for films on R-plane and M-plane sapphire substrates.

In Figure 6 it is evidenced that sharp transitions can be obtained from ultra-thin NbN layers grown on M-plane sapphire: T_c reaches 13.2 K uniformly across a 3-inch wafer, for a film thickness of 4.4 nm (measured by X-ray reflectivity) and 11.7 K for a 2.9 nm thick film.

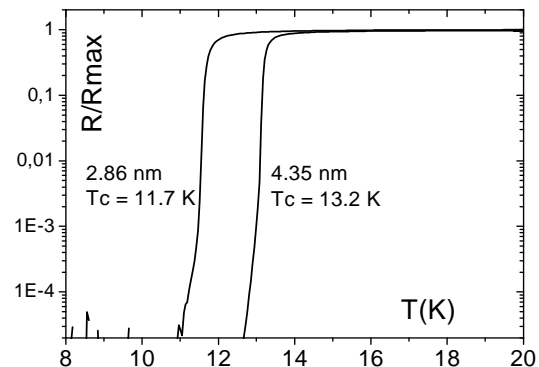


Fig. 6. Critical temperature observed as a function of normalized resistance for two NbN very thin films grown on an M-plane sapphire substrate.

Patterning and processing nanowires have been achieved to confirm that superconducting electronic devices relying on nano-wires would benefit from the more homogeneous properties of NbN grown on M-plane sapphire without significant process induced degradation.

The NbN film goes through a four-step low temperature process described elsewhere [17], which includes the deposition and e-beam lithography ($U=100$ kV, dose $105 \mu\text{C}/\text{cm}^2$) of a 150 nm thick NEB22 Sumitomo negative tone resist, followed by reactive ion etching in SF_6/O_2 to define the wires.

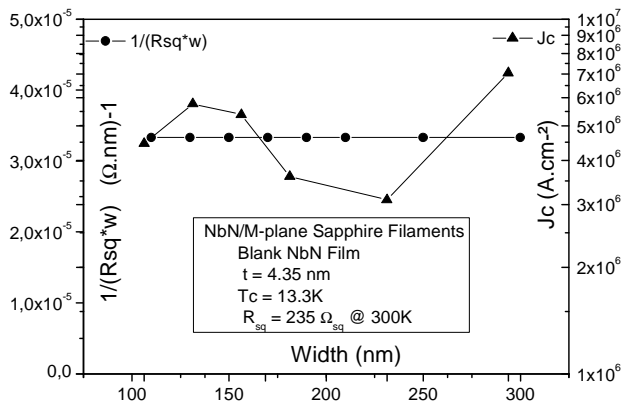


Fig. 7. Measurement of the NbN filaments conductivity at 300K and critical current density at 4.2K versus the filament width, after patterning.

Resist development was done in a Rohm and Haas MF702 for 45 s after a post-exposure bake of 90°C for 60s, and then rinsed in water for 180 s. Finally the stripping of the resist was completed using Dupont's EKC-LE solution. The obtained wire widths vary from 50 nm to 10 μ m, and are 30 μ m long. Figure 7 shows that filament conductivity does no more depend on the width of the patterned stripe down to 80 nm, thanks to the e-beam writers used. T_c and square resistance values are also maintained close to those of the un-patterned films grown on M-plane. Critical current density J_c was measured in a 3 to 7 MA/cm² range at 4.2K for the set of samples presented; the apparent variation observed should be due to some measurement imprecisions induced by using the field criteria $\sim 10\mu$ V/cm applied to different geometries.

V. EPITAXIAL NbN-MGO-NbN JOSEPHSON JUNCTIONS ON R-PLANE SAPPHIRE

Taking benefit of the high crystalline quality of very thin NbN layers on sapphire, we used them as a template for growing epitaxial SIS and SNS tri-layers. A 10 nm base-electrode seed was epitaxially grown at 600°C while subsequent deposition took place in the 250-400°C range for preventing the nucleation of the HCP phase of NbN. Junctions are patterned using the SNOP process described previously [15].

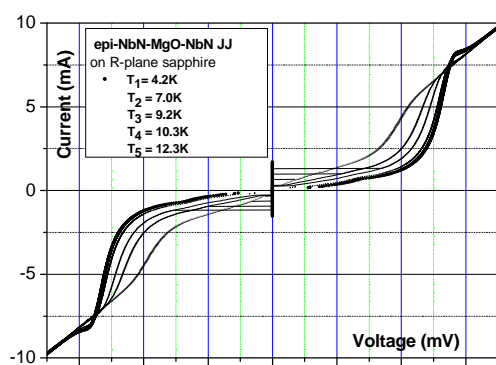


Fig.8. Current-Voltage characteristics between 4K and 12K of a NbN-MgO-NbN superconducting tunnel junction with 50nm thick NbN electrodes grown on R-plane sapphire. The gap voltage V_G observed at 5.3mV and 4.2K decrease down to 3.5mV at 12.3K.

RF-sputtered MgO (~ 1 nm thick) and Ta_xN (~ 7 nm thick) barriers are found cubic crystalline and well textured when

deposited at about 300°C. The Current-Voltage characteristics of a NbN-MgO-NbN SIS junction with 50nm thick electrodes made on R-plane sapphire is observed in Figure 8, in the 4K-12K range. The gap voltage V_G and Josephson current are observed up to 12.3K. Attractive photo-detection properties of such epitaxial thin electrodes junction are under investigation.

VI. CONCLUSION

Significant progress has been achieved by using the M-plane of sapphire in obtaining higher crystalline quality. Now, the reliability of ultra-thin NbN films and junctions deposited uniformly on 3 and 4 inch diameter sapphire wafers allows us to extend up to 8-inch diameter substrates. We plan further development of superconducting single photon detectors, THz HEB mixers based on NbN and also devices for low noise quantum analog and digital Josephson circuits.

ACKNOWLEDGMENT

We would like to thank S. Pouget and E. Bellet-Amalric from CEA-INAC SP2M for their support for XRD characterizations and interpretation. We also would like to thank L. Maingault and J-L. Thomassin of CEA-INAC SPSMS for their support at the PTA cleanroom for the e-beam patterning of NbN nanowires.

REFERENCES

- [1] R.T. Kampwirth, K.E. Gray, IEEE Trans. Mag. **17**, 1981, pp. 565-568.
- [2] A I Braginski and J Talvacchio, in Superconducting Devices, S T Ruggiero, D A Rudman, Boston, Academic Press 1990.
- [3] G N Gol'tsman, O. Okunev, G. Chulkova, A. Lipatov, A. Semenov, K. Smirnov, B. Voronov, A. Dzardanov, A. Williams, R. Sobolewski, Appl. Phys. Lett., vol. 79, 2001, pp. 705-707.
- [4] A. Divochiy, et al, Nature Photonics, vol. 2, no. 5, 2008, pp. 302-306.
- [5] E. le Coarer et al, Nature Photonics, vol. 1, no. 8, 2007, pp. 473-478.
- [6] J R Gao, M Hajenius, F D Tichelaar, T M Klapwijk, B Voronov, E Grishin, G N Gol'tsman, C A Zorman, M Mehregany, Appl. Phys. Lett. Vol. 91, 2007, pp. 062504-062506.
- [7] G. L. Kerber, L. A. Abelson, R. N. Elmadjian, E. G. Ladizinsky, , IEEE Trans. Appl. Supercond. 9 - 2, 1999, pp. 3267-3270.
- [8] Z. Wang, A. Kawakami, Y. Uzawa, B. Komiyama, J. Appl. Phys., vol. 79, 1996, pp. 7837-7844.
- [9] A.B. Kaul, S.R. Whiteley, T. Van Duzer, L. Yu, N. Newman, J.M. Rowell, Appl. Phys. Lett. 78, 2001, pp. 99-101.
- [10] J-C Villegier et al. *IEEE Trans. Appl. Supercond.* vol. 11(1), 2001, pp. 68-71.
- [11] A.J. Kerman et al, Appl. Phys. Lett. Vol. 90, 2007, pp. 101110-101112.
- [12] R. Espiau de Lamaestre, Ph. Odier, J-C Villegier, Appl. Phys. Lett. Vol. 91, 2007, pp. 232501-232503.
- [13] R. Espiau de Lamaestre, Ph. Odier, E. Bellet-Amalric, P. Cavalier, S. Pouget, J-C. Villegier, Journal of Physics: Conference Series vol. 97, 2008, pp 012046-012052.
- [14] V.L. Noskov et al, Sov. Phys. Crystallogr. Vol. 25(4), 504, (1980),
- [15] R. Setzu, E. Baggetta, J-C. Villegier, Journal of Physics: Conference Series, vol. 97, 2008, 012077.
- [16] L. G. Paratt, Phys. Rev., vol.95, 1954, pp. 359
- [17] C. Constancias et al, vol. 25, no. 6. AVS, 2007, pp. 2041-2044.
- [18] P. Ruterana et al, to be published.
- [19] C. Jorel et al, to be published.